

Simple renormalization-group approximation of the ground-state properties of interacting bosonic systems

Roman Werpachowski*

Center for Theoretical Physics PAS, Aleja Lotników 32/46, 02-668 Warsaw, Poland

Jerzy Kijowski

Center for Theoretical Physics PAS, Aleja Lotników 32/46, 02-668 Warsaw, Poland and Cardinal Stefan Wyszyński University in Warsaw, Warsaw, Poland

(Received 19 March 2007; revised manuscript received 18 April 2007; published 21 June 2007)

We present a simple renormalization-group method of investigating ground-state properties of interacting bosonic systems. Our method reduces the number of particles in a system, which makes numerical calculations possible for large systems. It is conceptually simple and easy to implement, and allows investigation of properties unavailable through mean-field approximations, such as one- and two-particle reduced density matrices of the ground state. As an example, we model a weakly interacting one-dimensional Bose gas in a harmonic trap. Compared to the mean-field Gross-Pitaevskii approximation, our method provides a more accurate description of the ground-state one-particle density matrix. We have also obtained the Hall-Post lower bounds for the ground-state energy of the gas. All results have been obtained by straightforward numerical diagonalization of the Hamiltonian matrix.

DOI: [10.1103/PhysRevA.75.062113](https://doi.org/10.1103/PhysRevA.75.062113)

PACS number(s): 03.65.Ge, 05.10.Cc, 67.40.Db

I. INTRODUCTION

The numerical investigation of the ground-state properties of a multiparticle interacting bosonic system is a much harder task than in the case of a single-particle system. The naive approach consists in choosing a large enough finite Hilbert space basis and the numerical diagonalization of the resulting Hamiltonian matrix. However, the necessary basis size grows exponentially with the number of particles, which makes this simple method inadequate for the treatment of large systems. To avoid this problem, many approximations have been invented, such as the Gross-Pitaevskii (GP) mean-field approach [1,2], the density-matrix renormalization-group (DMRG) method [3,4], or, in the case of strong interactions, the Thomas-Fermi approximation [1] and the Tonks-Girardeau model [5,6]. For fermionic systems, the exact diagonalization *ab initio* method (EDABI) has been implemented [7–9]. One should also note the exceptional case of a full analytical solution in one dimension by Lieb and Liniger [10]. From this solution, two- and three-pair correlation functions of an interacting one-dimensional (1D) Bose gas have been derived [11–13]. In this paper we present a different approach, which has similarities to renormalization-group methods but is conceptually simple and easy to implement. Our method amends the problem of unmanageable basis size by reducing the number of particles in the system and renormalizing the Hamiltonian. We approximate the one- and two-particle properties of the large system using the same properties of the smaller system. In contrast to mean-field methods, our approach allows calculation of such quantities as one- or two-particle reduced density matrices (1-RDMs and 2-RDMs) of the ground state.

In Sec. II, we describe how our method works. Section III contains an example application of the method to the prob-

lem of a one-dimensional interacting Bose gas in a harmonic trap. The results are summarized in Sec. IV.

II. HAMILTONIAN RENORMALIZATION AND THE APPROXIMATION OF GROUND-STATE PROPERTIES

We present our approximation in the case of a system with two-body interactions. It can be easily generalized to the general case of n -body interactions.

Consider a 1D Hamiltonian describing a system of N scalar (zero-spin) bosons,

$$\hat{H}_N = \sum_{k=1}^N \left(-\frac{\hbar^2}{2m} \frac{\partial^2}{\partial x_k^2} + V_1(x_k) \right) + \sum_{k=1}^N \sum_{k'=1}^{k-1} V_2(x_k, x_{k'}), \quad (1)$$

where N is the number of particles, m is the particle mass, $V_1(x)$ is the external one-particle potential, and $V_2(x, x') = V_2(x', x)$ is the two-particle interaction potential.

When investigating such a system, we are often interested only in one- or two-particle properties of the ground state. One way to calculate them is to obtain an approximation of the 1-RDM or 2-RDM of the ground state.

We approximate the system by replacing it with a much smaller system containing $N' \ll N$ scalar bosons. The smaller system is governed by a renormalized version of the original Hamiltonian \hat{H}_N , that is,

$$\hat{H}_{N'} = \frac{N}{N'} \left[\sum_{k=1}^{N'} \left(-\frac{\hbar^2}{2m} \frac{\partial^2}{\partial x_k^2} + V_1(x_k) \right) + \frac{N-1}{N'-1} \sum_{k=1}^{N'} \sum_{k'=1}^{k-1} V_2(x_k, x_{k'}) \right]. \quad (2)$$

We calculate the properties of interest from the ground state

*Corresponding author: roman@cft.edu.pl

of $\hat{H}_{N'}$, thus avoiding the insurmountable problem of diagonalizing the Hamiltonian of the large system, \hat{H}_N . The results for increasing values of N' will converge to the values of the corresponding properties of the N -particle system.

We will now justify our procedure. Let Ψ and ρ be a state of the large system and its N' -RDM, respectively. It is easy to show that their mean energies, measured by the respective Hamiltonians, are equal,

$$\text{Tr}(\hat{H}_{N'}\rho) = \langle \Psi | \hat{H}_N | \Psi \rangle. \quad (3)$$

Hence, when the mean energy of Ψ becomes lower, moving closer to the mean energy of the ground state Ψ_0 of \hat{H}_N , the mean energy of ρ also becomes lower and moves closer to the mean energy of the (pure-state) density matrix ρ'_0 of the ground state Ψ'_0 of $\hat{H}_{N'}$. Because of the variational principle, the density matrix ρ'_0 is an approximation of the reduced density matrix ρ_0 of the ground state Ψ_0 . The one- or two-particle properties of ρ_0 (i.e., of Ψ_0), like the probability density, are approximated by the same properties of ρ'_0 (i.e., of Ψ'_0). Since $N' \ll N$, it is much easier to calculate numerically the ground state Ψ'_0 than the ground state Ψ_0 , and to investigate the one- or two-particle properties of Ψ_0 by investigating the same properties of Ψ'_0 .

The main source of error in our method is the fact that the variational search for the ground state converges to the N' -particle ground state Ψ'_0 , not to the RDM of the N -particle ground state, ρ_0 . This is because, for bosons, not every N' -particle density matrix is a RDM of an N -particle state. A better strategy would be to perform the variational search not in the whole N' -particle Hilbert space but in the smaller space of N' -particle density matrices which are RDMs of N -particle states. However, the problem of identifying this space, the so-called N -representability problem [14–16], remains unsolved. Therefore, we have to perform our calculations for a sequence of N' . The energy of the N' -particle ground state is a lower bound of the energy of the investigated N -particle ground state [17]. When N' increases, the ground state energy increases and approaches the ground state energy of the N -particle ground state. Due to the variational principle, this means that the N' -particle ground states approximate the N -particle ground state increasingly well, in the sense that the one- and two-particle properties calculated from these ground states converge to the corresponding properties of the N -particle ground state.

In the general case of n -particle interactions, the renormalization goes as follows: an n -particle interaction potential term $\sum_{k_1=1}^N \sum_{k_2=1}^{k_1-1} \dots \sum_{k_n=1}^{k_{n-1}-1} V_n(x_1, \dots, x_n)$, symmetrical with respect to permutations of coordinates x_k , is replaced by the term $\{[N(N-1) \dots (N-n+1)]/[N'(N'-1) \dots (N'-n+1)]\} \sum_{k_1=1}^{N'} \sum_{k_2=1}^{k_1-1} \dots \sum_{k_n=1}^{k_{n-1}-1} V_n(x_1, \dots, x_n)$. Equation (3) is true also in this general case.

III. A SIMPLE EXAMPLE

A. Investigated system

In our example, we consider a system of $N=100$ scalar bosons with a dimensionless Hamiltonian

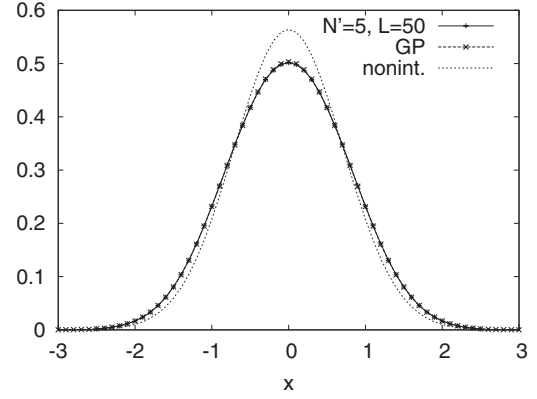


FIG. 1. Comparison of the probability densities obtained from our method (for $N'=5$ and $L=50$) and from the GP approximation, for $\lambda=10^{-2}$ (dimensionless units). The curves overlap perfectly, indicating convergence. The probability density of the noninteracting ($\lambda=0$) ground state is shown too. One can clearly see the difference between the interacting system and the noninteracting one, with the repulsive interaction pushing away the bosons in the trap.

$$\hat{H}_N = \sum_{k=1}^N \left(-\frac{1}{2} \frac{\partial^2}{\partial x_k^2} + \frac{1}{2} x_k^2 \right) + \lambda \sum_{k=1}^N \sum_{k'=1}^{k-1} \delta(x_k - x_{k'}),$$

where $\delta(x-x')$ is the Dirac δ function. This interaction potential is often used to describe cold bosons forming a Bose-Einstein condensate in a trap, when only s -wave scattering occurs [1]. Our example concerns positive λ , which lead to repulsive interaction.

We have approximated numerically the 1-RDM and 2-RDM of the ground state for two values of interaction strength λ . The procedure begins with the calculation of a finite matrix of the renormalized Hamiltonian $\hat{H}_{N'}$ in a finite basis composed of the noninteracting Hamiltonian ($\lambda=0$) eigenstates, permanents [19] of N' one-particle Hermite functions \mathcal{H}_k ,

$$\mathcal{H}_k(x) = \frac{1}{\sqrt{k!2^k\sqrt{\pi}}} H_k(x) \exp\left(-\frac{x^2}{2}\right), \quad (4)$$

where $H_k(x)$ is the k th Hermite polynomial. The basis contains all eigenstates with (nonrenormalized) energies lower

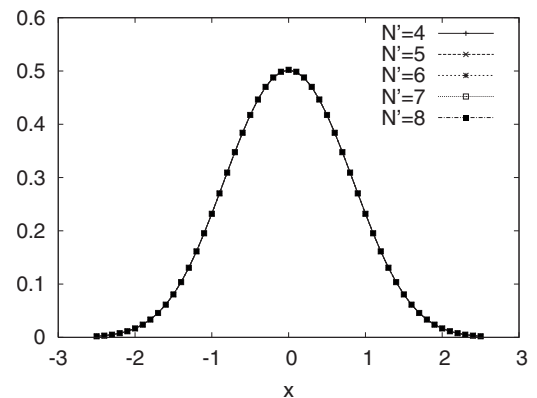


FIG. 2. Probability densities for $\lambda=10^{-2}$ calculated for increasing N' ($L=56, 50, 60, 40, 40$, respectively) in dimensionless units. The curves overlap perfectly, indicating convergence.

TABLE I. Bounds for the ground-state energy E_0 (dimensionless units). The first two, E_{GP} and E_{Gauss} , are the upper bounds calculated from the GP approximation and the variational method with a Gaussian wave function, respectively. The last one, E_{HP} , is the Hall-Post lower bound, which is provided by our method as an estimate of the true ground-state energy.

λ	E_{GP}	E_{Gauss}	E_{HP}
10^{-2}	68.8	68.9	68.2
5×10^{-2}	130.9	132.3	121.4

than a cutoff energy $L+N'/2$, i.e., permanents of functions \mathcal{H}_{k_n} , $n=1, \dots, N'$, such that $\sum_{n=1}^{N'} k_n < L$. Then, the ground state is calculated with the help of an iterative Lanczos-type numerical procedure [18]. From the ground state we obtain the 1-RDM and the 2-RDM, with trace normalized to unity. Using them, we can calculate any one- or two-particle property of the ground state. For given N' , the basis cutoff L is chosen to be large enough so that calculated properties do not change upon further increase of L .

In the case of the 1-RDM ρ_1 , we compare the diagonal part $\rho_1(x, x)$ with the probability density calculated by minimizing numerically the GP energy functional [1] of our system,

$$E[\Psi] = \frac{N}{2} \int_{-\infty}^{\infty} \left[\Psi^*(x) \left(-\frac{\partial^2}{\partial x^2} + x^2 \right) \Psi(x) + (N-1)\lambda |\Psi(x)|^4 \right] dx. \quad (5)$$

The minimization is performed by expanding the wave function $\Psi(x)$ in the finite basis of the first 20 Hermite functions (4), inserting the expansion into (5), and minimizing numerically the resulting functional of the expansion coefficients.

We present numerical results for two values of λ , 10^{-2} , and 5×10^{-2} . Both values are in the regime of weak interactions, where the minimization of the GP energy functional provides a good approximation of the ground state. All numerical values are given in dimensionless units.

B. Ground-state energy

First, we provide the data for the ground-state energy E_0 . In the noninteracting case $\lambda=0$, E_0 is precisely known and equals 50. Table I lists three different approximations of E_0 for two nonzero values of λ . In the second and third columns of Table I, two different upper bounds for E_0 are listed: the one obtained from the GP functional, E_{GP} , and the variational bound, E_{Gauss} , calculated as a minimal mean value of \hat{H}_N in the state Ψ_σ , a product of N Gaussian one-particle wave functions with a common variational parameter σ ,

$$\Psi_\sigma(x_1, \dots, x_N) = \prod_{k=1}^N \frac{1}{\sqrt{2\pi\sigma^2}} \exp\left(-\frac{x_k^2}{4\sigma^2}\right),$$

i.e., $E_{\text{Gauss}} = \min_{\sigma \in \mathbb{R}} \langle \Psi_\sigma | \hat{H}_N | \Psi_\sigma \rangle$. Relatively small differences between E_{GP} and E_{Gauss} indicate that the ground states

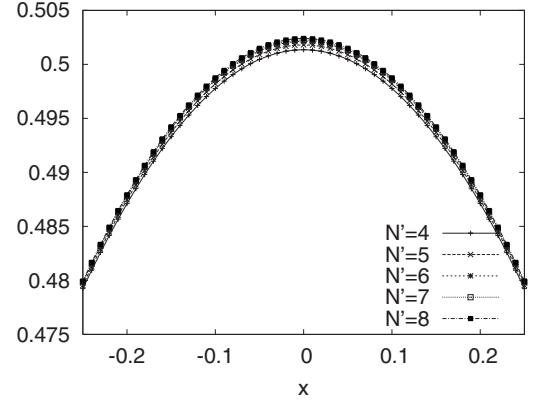


FIG. 3. Probability densities for $\lambda=10^{-2}$ calculated for increasing N' ($L=56, 50, 60, 40, 40$, respectively), shown in the range $x \in [-0.25, 0.25]$ (dimensionless units). The plot has been magnified in order to show the details of the convergence.

are close to Gaussian. As expected, the GP approximation provides a better estimation of the ground-state energy than the Gaussian ansatz. Our method provides an estimation of the true ground-state energy E_0 as the so-called Hall-Post [17] lower bound E_{HP} . Values of E_{HP} are listed in the fourth column of Table I. They were calculated by nonlinear least squares fitting of the ground-state energy for fixed N' (in our calculations, we have used results for $N'=8$, so as to make E_{HP} as high as possible) as a function of L to a power law

$$E(L) = E_{\text{HP}} + BL^C, \quad C < 0,$$

and taking the $L \rightarrow \infty$ limit, obtaining E_{HP} as the answer. It has been necessary to follow this procedure, since raw numerical results vary with L , even for L large enough so that the 1-RDM does not change. The relative asymptotic standard error of the fitting procedure is below 0.01% for both values of λ .

The bounds on E_0 (E_{HP} and E_{GP}) presented above are quite close. The relative uncertainty with which E_0 is deter-

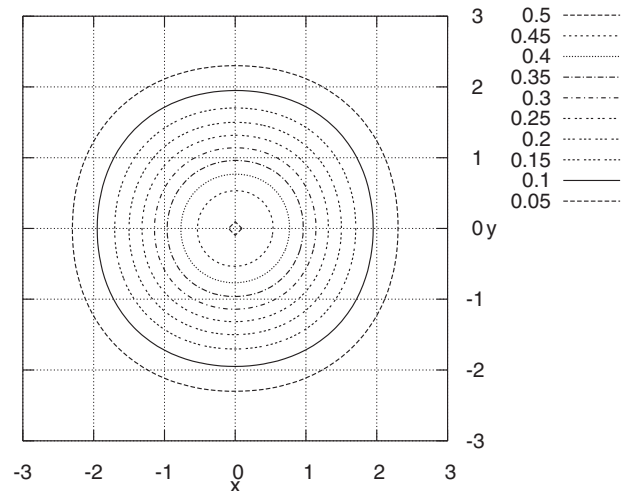


FIG. 4. Contour plot of $\rho_1(x, y)$ for $\lambda=10^{-2}$, calculated for $N'=5$ and $L=50$ (dimensionless units). Isolines display a radial symmetry.

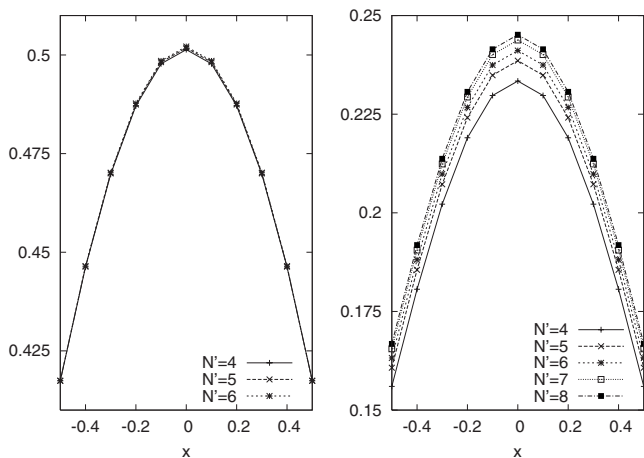


FIG. 5. On the left plot, the probability density $\rho_1(x,x)$ for $\lambda = 10^{-2}$ is shown for increasing N' ($L=56, 50, 60$, respectively) in dimensionless units. The curves converge quickly. On the right plot, the diagonal part of the 2-RDM, $\rho_2(x,x,x,x)$, is plotted (for the same λ) for increasing N' ($L=56, 50, 60, 40, 40$, respectively). Even for $N'=7$ or 8, the curves do not converge.

mined by them is below 1% for $\lambda = 10^{-2}$ and around 8% for $\lambda = 5 \times 10^{-2}$. (We have calculated the relative uncertainty as the ratio of the difference between the upper and the lower bound to the lower bound.) The fact that it is small supports the applicability of our approximation, as it means that the true ground-state energy is also close to the obtained lower bound. On the other hand, if the reduced density matrix of the N' -particle ground state Ψ'_0 is to be a good approximation of the reduced density matrix of the true ground state, the mean energy of Ψ'_0 —i.e., the Hall-Post lower bound—must be close to the true ground-state energy of the system. Our results satisfy this condition.

C. Density matrices

For $\lambda = 10^{-2}$, we obtain identical one-particle probability densities from our method and from the GP approximation, as shown on Fig. 1. The accuracy of our approximation is

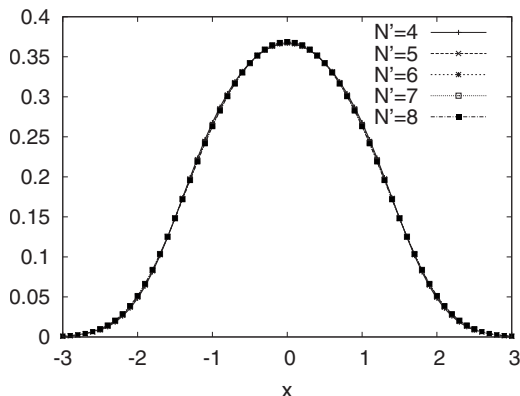


FIG. 6. Convergence of the probability densities $\rho_1(x,x)$ for $\lambda = 5 \times 10^{-2}$ and increasing values of N' ($L=55, 50, 60, 40, 40$, respectively) in dimensionless units. The curves overlap, indicating convergence.

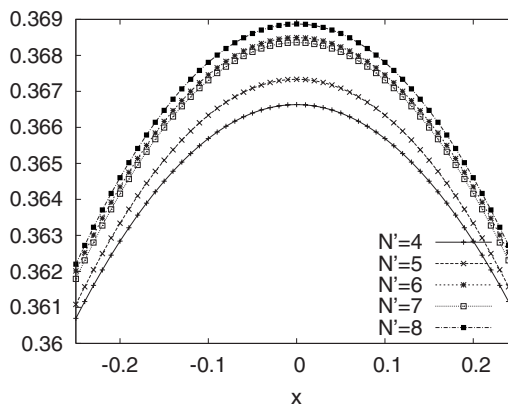


FIG. 7. Probability densities for $\lambda = 5 \times 10^{-2}$ calculated for increasing N' ($L=55, 50, 60, 40, 40$, respectively), shown in the range $x \in [-0.25, 0.25]$ (dimensionless units). The plot has been magnified in order to show the details of the convergence.

confirmed by Fig. 2, which shows that different values of N' and L yield identical probability densities. A magnified section of this plot is shown in Fig. 3. We will use the convergence with increasing N' as a benchmark of the accuracy of our method, treating our numerical results as correct if they stabilize quickly. For each N' , we take the results for L large enough so that they do not change upon further increase of L . A similar convergence occurs for the antidiagonal part of the 1-RDM, $\rho_1(x, -x)$.

The GP approximation, however, cannot provide us with knowledge about the nondiagonal parts of the 1-RDM. The merit of our method is that we can calculate $\rho_1(x,y)$ for any (x,y) . For $\lambda = 10^{-2}$, we obtain numerically

$$\rho_1(x,y) \approx \rho_1(\sqrt{x^2 + y^2}), \tag{6}$$

which is clearly shown by the contour plot of $\rho_1(x,y)$ in Fig. 4.

The convergence of the diagonal part of the 1-RDM, $\rho_1(x,x)$ and of the diagonal part of the 2-RDM, $\rho_2(x,x,x,x)$

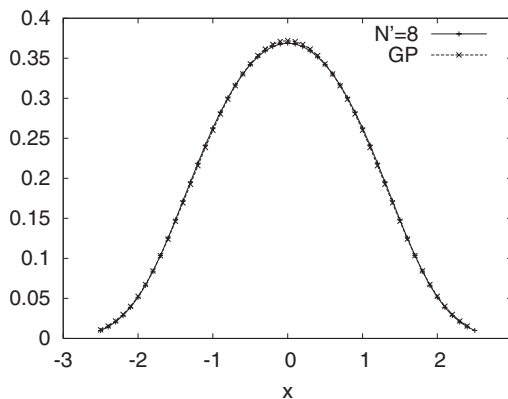


FIG. 8. Probability density for $\lambda = 5 \times 10^{-2}$, as calculated with our method ($N'=8$ and $L=40$) and from the minimization of the GP functional (dimensionless units). A slight difference between the two curves can be seen in the middle of the plot, indicating that interactions are strong enough so that the GP approximation results differ from ours.

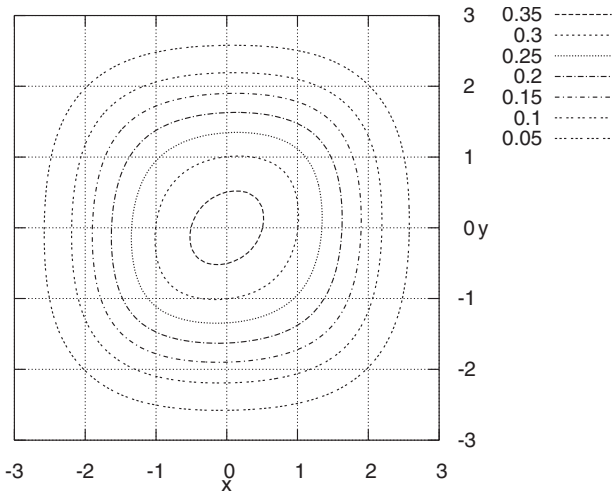


FIG. 9. Contour plot of $\rho_1(x,y)$ for $\lambda=5 \times 10^{-2}$, calculated for $N'=8$ and $L=40$ (dimensionless units). Isolines do not display radial symmetry, unlike for $\lambda=10^{-2}$.

(the probability of finding both particles in the same position x), is compared in Fig. 5. It is clear that the convergence, with increasing N' , of the second function is much slower. The consequence of this is that using only such simple diagonalization techniques as we did, which limit us to $N' < 10$, we cannot estimate the 2-RDM, even for λ as small as 10^{-2} .

For $\lambda=5 \times 10^{-2}$, we obtain the convergence of the probability densities as easily, as for $\lambda=10^{-2}$ (see Fig. 6), although it is slightly slower (not visible on the plot). A magnified section of this plot is shown in Fig. 7. A similar convergence occurs for the antidiagonal part of the 1-RDM, $\rho_1(x,-x)$. However, the probability density differs slightly from the one obtained from the GP functional, as seen in Fig. 8. Contrary to the case of $\lambda=10^{-2}$, the contour plot of the 1-RDM for $\lambda=5 \times 10^{-2}$ is no longer radially symmetric, as can be seen on Fig. 9. It differs noticeably from the one (shown in Fig. 10) we would obtain from the mean-field

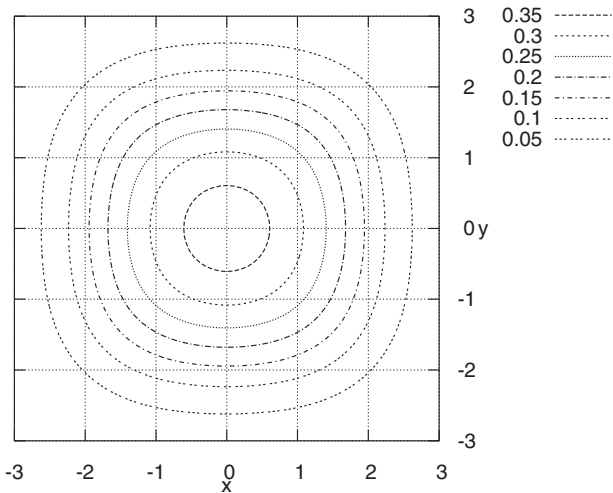


FIG. 10. Contour plot of $\rho_1(x,y)$ calculated for $\lambda=5 \times 10^{-2}$ using the GP approximation (dimensionless units). It is clearly visible that this plot is more symmetrical than the one in Fig. 9.

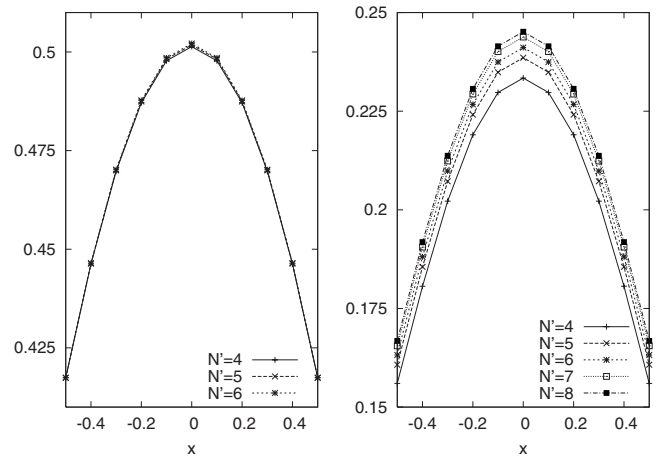


FIG. 11. Left panel: Probability density $\rho_1(x,x)$ for $\lambda=10^{-2}$ for increasing N' ($L=56,50,60$, respectively) in dimensionless units. Right panel: Same quantity for $\lambda=10^{-1}$ ($L=55,50,60$, respectively). The convergence for the higher value of λ is visibly slower.

method, using the formula

$$\rho_1(x,y) \approx \Psi_{GP}(x)\Psi_{GP}(y),$$

where Ψ_{GP} is the real wave function that minimizes the GP energy functional. This difference is the most striking result in this section, and indicates that our method gives more accurate results than mean-field approximations.

For an even higher value of λ , 10^{-1} , we did not obtain fast enough convergence of either $\rho_1(x,x)$ (see Fig. 11) or, especially, $\rho_1(x,-x)$ (see Fig. 12). This prevented us from investigating the full 1-RDM for this interaction strength. We conclude that $\lambda=10^{-1}$ is outside the range of our approximation in its present form. To reach this interaction strength, we would have to calculate the density matrices of the N' -particle ground state for N' higher than those treatable with the simple numerical diagonalization algorithm used by us.

IV. SUMMARY

We have presented a method of investigating one- and two-particle reduced density matrices of the ground state of

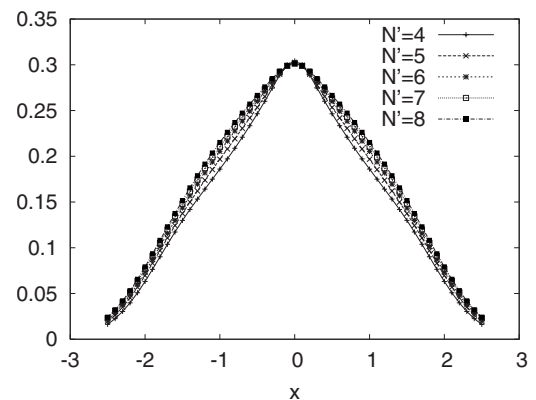


FIG. 12. Antidiagonal part of 1-RDM for $\lambda=10^{-1}$ for increasing N' ($L=55,50,60,39,40$, respectively) in dimensionless units. Convergence is too slow for the results to be meaningful.

an interacting system with a large number of bosonic particles. The method approximates it with a smaller, renormalized system. It is conceptually simple and easy to implement numerically. The results it provides would be, for high enough interaction strengths (e.g., $\lambda=5 \times 10^{-2}$ in our example), impossible to calculate using mean-field methods, such as the GP approximation.

We have provided an example application of our method to the problem of a one-dimensional interacting Bose gas in a harmonic trap, obtaining accurate approximations of a quantity unobtainable from mean-field methods, namely, the full one-particle density matrix. The results are precise and accurately describe the large system, which is proven by the fact the the results converge quickly with increasing N' . The GP approximation does not give as accurate a picture of the ground-state one-particle density matrix as our approach. Additionally, the Hall-Post lower bounds for the ground-state

energy have been calculated. The relatively small difference between them and the upper bounds (GP and Gaussian) also supports the applicability of our method.

Even using simple numerical procedures, our method gives access to properties that were previously not as accurately described by mean-field methods. To investigate the two-particle density matrix, or to perform simulations of systems with higher interaction strengths, would require the use of more refined approaches to the calculation of the ground state of the renormalized Hamiltonian, for example the DMRG [3,4] or the EDABI [7–9] method.

ACKNOWLEDGMENTS

The authors want to thank Professor Iwo Białynicki-Birula and Professor Kazimierz Rzążewski for helpful discussions and advice.

-
- [1] L. P. Pitaevskii and S. Stringari, *Bose-Einstein Condensation* (Oxford University Press, Oxford, 2003).
- [2] F. Dalfovo, S. Giorgini, L. P. Pitaevskii, and S. Stringari, *Rev. Mod. Phys.* **71**, 463 (1999).
- [3] S. R. White, *Phys. Rev. Lett.* **69**, 2863 (1992).
- [4] U. Schollwöck, *Rev. Mod. Phys.* **77**, 259 (2005).
- [5] L. Tonks, *Phys. Rev.* **50**, 955 (1936).
- [6] M. Girardeau, *J. Math. Phys.* **1**, 516 (1960).
- [7] J. Spałek, R. Podsiadły, W. Wójcik, and A. Rycerz, *Phys. Rev. B* **61**, 15676 (2000).
- [8] A. Rycerz and J. Spałek, *Phys. Rev. B* **63**, 073101 (2001).
- [9] J. Spałek and A. Rycerz, *Phys. Rev. B* **64**, 161105(R) (2001).
- [10] E. H. Lieb and W. Liniger, *Phys. Rev.* **130**, 1605 (1963).
- [11] K. V. Kheruntsyan, D. M. Gangardt, P. D. Drummond, and G. V. Shlyapnikov, *Phys. Rev. Lett.* **91**, 040403 (2003).
- [12] K. V. Kheruntsyan, D. M. Gangardt, P. D. Drummond, and G. V. Shlyapnikov, *Phys. Rev. A* **71**, 053615 (2005).
- [13] D. M. Gangardt and G. V. Shlyapnikov, *Phys. Rev. Lett.* **90**, 010401 (2003).
- [14] A. J. Coleman, *Rev. Mod. Phys.* **35**, 668 (1963).
- [15] M. B. Ruskai, *Phys. Rev.* **183**, 129 (1969).
- [16] G. Gidofalvi and D. A. Mazziotti, *Phys. Rev. A* **69**, 042511 (2004).
- [17] R. L. Hall and H. R. Post, *Proc. Phys. Soc. London* **90**, 381 (1967).
- [18] R. Lehoucq, K. Maschhoff, D. Sorensen, and C. Yang, computer code ARPACK, <http://www.caam.rice.edu/software/ARPACK/>
- [19] A permanent is the bosonic counterpart of the Slater determinant. For example, for two particles the wave function $\Psi(x_1, x_2) \sim \psi_a(x_1)\psi_b(x_2) + \psi_b(x_1)\psi_a(x_2)$ is the permanent of one-particle wave functions ψ_a and ψ_b .